

**INVESTIGATION OF SHORT-CIRCUIT ELECTROMAGNETIC
FORCE IN THREE-PHASE BUSBAR SYSTEM**

FARHANA BINTI MOHAMAD YUSOP

**UNIVERSITI SAINS MALAYSIA
2013**

**INVESTIGATION OF SHORT-CIRCUIT ELECTROMAGNETIC FORCE IN
THREE-PHASE BUSBAR SYSTEM**

by

FARHANA BINTI MOHAMAD YUSOP

**Thesis submitted in fulfillment of the requirements
for the degree of
Master of Science**

July 2013

ACKNOWLEDGEMENTS

There are many individuals whom I would like to thank for their underlying support and guidance that made it possible for me to complete this thesis.

First of all, my sincere gratitude goes to my supervisor Dr. Mohamad Kamarol and my co-supervisor, Dr. Dahaman Ishak for their extremely knowledgeable advices, tips and encouragement that help me a lot in staying on the right track for this research.

I owe a debt of gratitude to my parents for their continuous support and encouragement especially for the sacrifice that they have made while I completed this thesis.

I would like to thank and appreciation to the USM Fellowship Scheme for its financial support and also thanks to Furutec Electrical Sdn. Bhd for this good collaborative project during my study. Without this support I will not be able to manage my financial properly.

Last but not least, I wish to express my special thanks to all my fellow friends for their guidance and contribution. I offer my regards and blessings to all of those who supported me in any respect during the completion of the project

TABLE OF CONTENTS

	Page
ACKNOWLEDGEMENT	ii
TABLE OF CONTENTS	iii
LIST OF TABLES	vi
LIST OF FIGURES	viii
LIST OF SYMBOLS	xii
LIST OF ABBREVIATION	xiv
ABSTRAK	xv
ABSTRACT	xvii
CHAPTER 1 – INTRODUCTION	
1.1. Overview of the Project	1
1.2. Problem Statement	4
1.3. Objective	5
1.4. Scope of Research	5
1.5. Structure of Thesis	6
1.6. Contribution	7
CHAPTER 2 – LITERATURE REVIEW	
2.1. Introduction	8
2.2. Research Trend on Electromagnetic Force due to Short-circuit Current	8
2.3. Related Theory of Short-circuit Current	13
2.3.1. Three-phase Short-circuit Current	13
2.3.2. Initial Symmetrical Short-circuit Current I''_k	14

2.3.3.	Peak Short-circuit Current i_p	15
2.3.4.	Development of Three-phase Short-circuit Current	17
2.4.	Electromagnetic Force Affected by Short-circuit Current	20
2.4.1.	Computational of Electromagnetic Force	20
2.4.2.	Calculation of Electromagnetic Force Based on IEC Standards 60865-1	23
2.4.3.	Proximity Effect of Inductive Material – Enclosure	25
2.5.	Summary	26
CHAPTER 3 – METHODOLOGY		
3.1.	Introduction	31
3.2.	Introduction of Opera-2D	31
3.3.	Process Flow of the Research Work	32
3.4.	Electromagnetic Force under Steady-state Short-circuit AC Current	33
3.4.1.	Calculation of Three-phase Short-circuit Current	35
3.4.2.	Calculation of Impedance of Busbar System	36
3.4.3.	Calculation of Peak Three-phase Short-circuit Current	38
3.4.4.	Structure of Rigid Bare Conductor Busbar	40
3.4.5.	Evaluation of Skin Depth	43
3.5.	Electromagnetic Force under Transient Three-phase Short-circuit Current	43
3.5.1.	Development of Transient Short-circuit Current	44
3.5.2.	Model of 3-phase 5-wire (3P5W) Busbar System	48
3.5.3.	Estimation of Short-circuit Electromagnetic Force	50
3.6.	Summary	54

CHAPTER 4 – RESULT AND DISCUSSION

4.1. Introduction	55
4.2. Evaluation of Electromagnetic Force under Steady-state Short-circuit Current	55
4.2.1. Effect of Dimensional Arrangement of Rigid Bare Conductor Busbar on Electromagnetic Force	60
4.3. Evaluation of Electromagnetic Force under Transient Three-phase Short-circuit Current	63
4.3.1. Effect of Dimensional Arrangement of 3P5W Conductor Busbar on Electromagnetic Force	76
4.3.2. Effect of Busbar Arrangement on Electromagnetic Force	81
4.3.3. Electromagnetic Force for Different Conductor Arrangement	82
4.4. Evaluation of Electromagnetic Force for Different Stack Busbar System	85
4.5. Validation of Computational Electromagnetic Force	87
4.6. Summary	94

CHAPTER 5 – CONCLUSION

5.1. Conclusion of the Project	100
5.2. Recommendations for Future Work	101

REFERENCES

APPENDICES

Appendix A : Getting Started with Opera-2D

Appendix B : Result of Electromagnetic Force with the Present of Insulating Material

Appendix C : Short-circuit Test Report

Appendix D : Result of Electromagnetic Force

LIST OF PUBLICATIONS

LIST OF TABLES

	Page	
Table 2.1	Voltage factor c according to IEC 60909-0	15
Table 2.2	Standard values for the factor n	16
Table 2.3	Summarize of previous relevant work	28
Table 3.1	Rated data of the equipment	36
Table 3.2	Value for Z_T , R_T and X_T	37
Table 3.3	Rating of bare conductor busbar	37
Table 3.4	Value of peak short-circuit current	39
Table 3.5	Dimension arrangement of busbar	41
Table 3.6	Electrical properties of material	43
Table 3.7	Rated for 3P5W busbar system with its dimension	47
Table 3.8	Dimension of busbar system	49
Table 4.1	Maximum electromagnetic force obtained from the calculation	56
Table 4.2	Simulation data short-circuit current for Model X, $i_p = 63.0$ kA	65
Table 4.3	Simulation data of short-circuit current for Model Y, $i_p = 73.5$ kA	67
Table 4.4	Simulation data of short-circuit current for Model Z, $i_p = 105.0$ kA	69
Table 4.5	Electromagnetic force at peak short-circuit current	74
Table 4.6	Electromagnetic force for EBACN arrangement	75
Table 4.7	Electromagnetic force for different arrangement of busbar system at peak short-circuit current	82
Table 4.8	Magnitude of electromagnetic force for different conductor arrangement	84
Table 4.9	Magnitude of electromagnetic force for different stack busbar system	86

Table 4.10	Dimension of conductor busbar for validation model	88
Table 4.11	Summary - maximum electromagnetic force obtained from calculation and simulation	94
Table 4.12	Summary - maximum electromagnetic force with varying conductor thickness, d	94
Table 4.13	Summary - maximum electromagnetic force with varying central distance, a	95
Table 4.14	Summary - electromagnetic force for 3P5W busbar at peak short-circuits current	95
Table 4.15	Summary - electromagnetic force with varying conductor width, b - $i_p = 73.5$ kA	95
Table 4.16	Summary - electromagnetic force with varying conductor thickness, d of 3P5W busbar	96
Table 4.17	Summary - electromagnetic force with varying spacing between conductor, a of 3P5W busbar	97
Table 4.18	Summary - electromagnetic force in different arrangement of 3P5W busbar	97
Table 4.19	Summary - electromagnetic force for different conductor arrangement of 3P5W busbar	98
Table 4.20	Summary - electromagnetic force for different stack busbar system	98
Table 4.21	Summary - comparison result of electromagnetic force for validation purpose	98

LIST OF FIGURES

		Page
Figure 1.1	Effect of short-circuit electromagnetic force on busbar system i. Busbar system before short-circuit test ii. Deformation on enclosure iii. Break down of supporting structure	3
Figure 2.1	Equivalent circuit for a three-phase short-circuit	14
Figure 2.2	Factor k for the calculation of peak short-circuit currents	16
Figure 2.3	Time behavior of short-circuit current	17
Figure 2.4	Equivalent single-phase diagram on three-phase short circuit current	18
Figure 2.5	Range of applicability of short-circuit calculation	19
Figure 2.6	Effect of electromagnetic force acting on parallel current carrying conductor	21
Figure 2.7	Variation of k_{1s} as a function of ratios a/d and b/d	23
Figure 2.8	Cross-section of bare conductor busbar	24
Figure 2.9	Effect of electromagnetic force produced on conductor A and B due to the presence of inductive material	26
Figure 3.1	Flow chart for the whole research project	33
Figure 3.2	Flow chart of the electromagnetic force under steady-state short-circuits AC current analysis (Condition 1)	34
Figure 3.3	Single-line diagram of short-circuit test	35
Figure 3.4	Equivalent circuit of the system	38
Figure 3.5	Typical waveform of three-phase AC current	39
Figure 3.6	Arrangement of rectangular bare conductor busbar i. Vertical arrangement ii. Horizontal arrangement	40
Figure 3.7	Illustration to determine the value of k from S-shape curve	42
Figure 3.8	Typical waveform of three-phase transient short-circuit current	45

Figure 3.9	Equivalent circuits for a busbar system i. Single stack ii. Double stack iii. Triple stack	46
Figure 3.10	3P5W busbar system i. Full view ii. Dimensional arrangement of conductor busbar	48
Figure 3.11	Actual design of 3P5W busbar system	49
Figure 3.12	Model of 3P5W single stack busbar system in different arrangement i. Horizontal arrangement ii. Vertical arrangement	51
Figure 3.13	Model of busbar for different conductor arrangement i. EABCN ii. NABCE iii. ENABC iv. NEABC v. ABCNE vi. ABCEN	51-52
Figure 3.14	Model of 3P5W busbar system for different stack arrangement i. Double stack ii. Triple stack	52
Figure 3.15	Flow-chart for transient analysis	47
Figure 4.1	Steady-state short-circuit AC current	57
Figure 4.2	Electromagnetic force per unit length in first half cycle of short-circuit current for vertical arrangement of conductor busbar	57
Figure 4.3	Distribution of magnetic flux density for vertical arrangement of conductor busbar i. at $\omega t = 0^\circ$ ii. at $\omega t = 60^\circ$	58
Figure 4.4	Result of maximum electromagnetic force for calculation and simulation under steady-state short-circuit current	59
Figure 4.5	Maximum electromagnetic force with varying conductor thickness i. Conductor of phase A ii. Conductor of phase B iii. Conductor of phase C	60-61

Figure 4.6	Maximum electromagnetic force with varying central distance between conductors i. Conductor of phase A ii. Conductor of phase B iii. Conductor of phase C	62-63
Figure 4.7	Three-phase short-circuit current from simulation i. Model X ii. Model Y iii. Model Z	64
Figure 4.8	Distribution of magnetic flux at peak short-circuit i. Model X ii. Model Y iii. Model Z	71-72
Figure 4.9	Electromagnetic force as a function of time under transient short-circuit current i. Model X ii. Model Y iii. Model Z	73
Figure 4.10	Model of busbar system with EBACN arrangement	75
Figure 4.11	Magnitude of electromagnetic force for $i_p = 73.5\text{kA}$ with varying conductor width, b	76
Figure 4.12	Magnitude of electromagnetic force with varying conductor thickness, d i. Model X – $i_p = 63\text{kA}$ ii. Model Y – $i_p = 73.5\text{kA}$ iii. Model Z – $i_p = 105\text{kA}$	77-78
Figure 4.13	Magnitude of electromagnetic force with varied spacing between conductors, a i. Model X – $i_p = 63\text{kA}$ ii. Model Y – $i_p = 73.5\text{kA}$ iii. Model Z – $i_p = 105\text{kA}$	79-80
Figure 4.14	Distribution of magnetic flux density for different busbar arrangements i. Vertical arrangement ii. Horizontal arrangement	82
Figure 4.15	Distribution of magnetic flux density for different conductor arrangement	83-84

Figure 4.16	Three-phase short-circuit current for different stack arrangement i. Double-stack – $i_p = 132\text{kA}$ ii. Triple-stack - $i_p = 110\text{kA}$	85-86
Figure 4.17	Busbar system for validation model i. Structure of busbar ii. Dimensional arrangement	87
Figure 4.18	Direction of short-circuit current i , magnetic flux density B and electromagnetic force F	89
Figure 4.19	Vector map of magnetic flux density from Opera-2D	89
Figure 4.20	Description Theory of Image for phase A conductor	90
Figure 4.21	Description Theory of Image for phase C conductor	91
Figure 4.22	Description Theory of Image for phase B conductor	92
Figure 4.23	Electromagnetic force for validation model at peak short-circuit current	93

LIST OF SYMBOLS

I_{k3}''	Three-phase short-circuit current
μ_0	Permeability of free space ($4\pi \times 10^{-7}$ H/m)
a	Central distance between two conductors
A	Cross-sectional area of conductor
a_m	Effective distance
B	Magnetic flux density
b	Width of rectangular conductor busbar
c	Voltage factor
d	Thickness of conductor busbar
F	Electromagnetic force
F_A, F_B, F_C	Magnitude of electromagnetic force
F_{ma}, F_{mb}, F_{mc}	Maximum electromagnetic force
I_A, I_B, I_C	Current
i_p	Peak short-circuit current
I_r	Rated current
I_{rms}	RMS current
J	Current density
k	Factor for calculation short-circuit current
k_{1s}	Correction factor for electromagnetic force
L	Inductance
l	Length of conductor
R	Resistance
t	Time
U_N	Nominal system voltage

V	Voltage
W	Conductor winding
X	Reactance
Z_T	Total impedance of the busbar system
α	Phase angle
τ	Time constant
ω	Angular frequency ($2\pi f$)

LIST OF ABBREVIATIONS

3P5W	Three-phase five-wire
A, B, C	Phase A, B, C conductor
AC	Alternative current
DC	Direct current
E	Earthing conductor
IEC	International Electrotechnical Commission
N	Neutral conductor
RMS	Root mean square
TR	Transient

KAJIAN DAYA ELEKTROMAGNETIK LITAR PINTAS DALAM SISTEM BUSBAR TIGA FASA

ABSTRAK

Sistem busbar adalah alat yang berkesan untuk mengedarkan elektrik sehingga beberapa kA dari bilik suis utama kepada beban. Oleh itu, ia haruslah disepadukan dengan ciri-ciri yang dikenal pasti yang boleh memberi keyakinan kepada pengguna untuk menggunakan sistem tersebut. Ujian litar pintas adalah salah satu ukuran yang amat penting bagi memastikan sistem busbar mampu untuk menampung daya elektromagnetik disebabkan arus litar pintas dalam tempoh masa tertentu. Setakat ini, pengeluar Malaysia terpaksa menghantar produk mereka keluar negara untuk melakukan ujian litar pintas disebabkan oleh ketidakupayaan negara untuk menyediakan kemudahan ujian litar pintas ini. Kos untuk melakukan ujian litar pintas ini amat tinggi dan memerlukan masa yang lama, dan ia akan terus meningkat jika produk mengalami kegagalan. Untuk mengatasi isu ini, kajian mengenai ramalan daya elektromagnetik disebabkan arus litar pintas adalah sangat diperlukan. Daya elektromagnetik pada konduktor busbar tegar disebabkan arus litar pintas dikira berpandukan IEC Standard 60865/93. Manakala, analisis unsur terhingga dilakukan untuk menganggarkan daya elektromagnetik ke atas sistem busbar. Analisis ini dipertimbangkan di bawah arus litar pintas keadaan mantap dan transien yang mana melibatkan 3P5W sistem busbar satu, dua dan tiga stack. Medan pengedaran magnet di analisis and prestasi sistem busbar dikenal pasti berdasarkan daya elektromagnetik yang dijanakan di bawah arus puncak litar pintas. Keputusan simulasi daya elektromagnetik telah menunjukkan prestasi yang baik dengan pengiraan. Analisis faktor seperti perubahan konfigurasi konduktor busbar dan ukuran dimensi sistem busbar dengan penambahan saiz sebanyak 1mm menghasilkan pengurangan daya

elektromagnetik ke atas konduktor sebanyak 3%-7%. Keputusan ini adalah panduan berguna untuk menentukan rekabentuk sistem busbar yang sesuai yang dapat menahan daya elektromagnetik kesan daripada arus litar pintas.

INVESTIGATION OF SHORT-CIRCUIT ELECTROMAGNETIC FORCE IN THREE-PHASE BUSBAR SYSTEM

ABSTRACT

Busbar system is an effective tool for distributing electricity up to a few kA from the main switch room to the load. Therefore, it should be integrated with a well-known characteristic that can give confidence to the consumer to use the distribution system. A short-circuit test is one of the very important parameters to ensure the system is able to withstand electromagnetic force due to short-circuit current for a definite time. Thus far, Malaysian manufacturers are compelled to send their products outside to do short-circuit tests due to Malaysia's inability to provide the facilities. The cost alone for performing short-circuit tests is considered high and take much time, and will continue to increase if the products having failure. To overcome this issue, studies on the prediction of electromagnetic force due to short-circuit current is highly necessary. Electromagnetic forces on rigid bare conductor busbars due to short-circuit currents are calculated based on IEC Standard 60865/93. Meanwhile, finite element analysis is performed in order to estimate the electromagnetic force on the busbar system. This analysis is considered under steady-state and transient short-circuit current which also involves a 3P5W of single, double and triple stack busbar system. The magnetic flux distributions are analyzed and the performance of the busbar system is identified based on the electromagnetic force generated under peak short-circuit currents. The simulation results of the electromagnetic force have shown good performance with numerical calculations. It is revealed that modification in the configuration of busbar conductor and dimensional arrangement of busbar system by an increment of 1mm result in a reduction of electromagnetic force on the conductors up to 3% -7%. This result is a

useful guideline for determining the appropriate designs of a busbar system that can withstand electromagnetic force affected by short-circuit current.

CHAPTER 1

INTRODUCTION

1.1. Overview of the Project

Busbar is used for the effective and efficient supply of electricity in most industrial locations. It is an effective tool for distributing electricity from a supply source to a few outgoing loads. Normally, a busbar consists of copper or aluminum conductors that can either be bare or insulated. It can carry currents up to a few kA from the main switch room to the loads. Nowadays, the busbar system has become very popular, and is widely utilized in industrial and residential applications due to its compactness and its requirement of a smaller space. Indeed, the demand on utilizing the busbar system in commercial, industrial and residential areas is relatively an increasing trend. As a result, numerous manufacturers compete to produce better quality and more reliable busbar systems for the market.

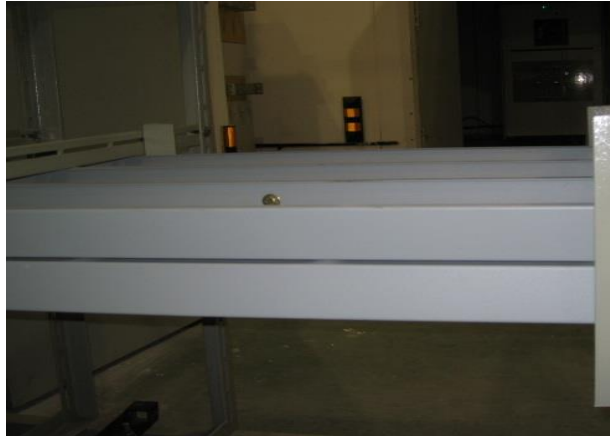
However, like other electrical power systems, a busbar may face some problems such as disaster damage and extensive downtime due to electrical faultiness. Faults due to short-circuits in the power system cannot be avoided despite careful planning and design, good maintenance and thorough operation of the system. According to Kasicki (2002), electrical equipment including busbar systems are subjected to electromagnetic force and thermal stress as a result of short-circuits which may damage the mechanical structure of the busbar system (Kasicki, 2002). Therefore, to keep the busbar system able to withstand the expected thermal and electromagnetic force, it must be designed appropriately.

There are various types of short-circuit that can arise in a three-phase busbar system (Kasikci, 2002; Schlabbach, 2005). The types of short-circuit currents are,

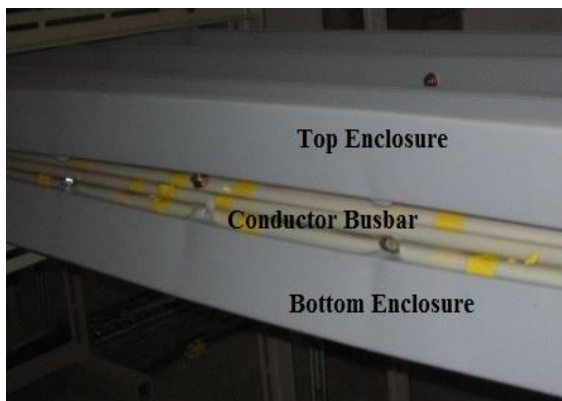
- i. Three-phase short-circuit
- ii. Line-to-line short-circuit without contact to ground
- iii. Line-to-line short-circuit with contact to ground
- iv. Single phase short-circuit

The effects of electromagnetic force on a parallel conductor busbar during a short-circuit current is of great interest. Extensively high current that is produced during short-circuit induces distractive forces between conductor busbars, especially in compact indoor installation where the distances are relatively small. In addition, the strength of electromagnetic force may also be influenced by the geometrical arrangement of the busbar system (Abd-El-Aziz, Adly, Essam-El-Din, & Abou-El-Zahab, 2004; Kasikci, 2002; Schlabbach, 2005)

The busbar under a short-circuit test may experience mechanical damage such as permanent deformation, break down of supporting structure and excess vibration stress on the busbar due to extremely higher electromagnetic force as shown in Figure 1.1. This damage is caused from the unpredicted electromagnetic force on a busbar system being sent to the short-circuit test laboratory. Thus, to avoid such situation from happening, the electromagnetic force and the busbar systems performance under short-circuit currents should be estimated before being sent to the laboratory for short-circuit tests. Determining the appropriate construction components of the busbar system and short-circuit electromagnetic force are important in order to control and avoid mechanical damage due to short-circuit currents. (Kasikci, 2002; Shah, Bedrosian, & Joseph, 1997).



(i) Busbar system before short-circuit test



(ii) Deformation on enclosure



(iii) Break down of supporting structure

Figure 1.1: Effect of short-circuit electromagnetic force on busbar system (courtesy of Furutec Electrical Sdn. Bhd)

Normally, the arrangement of parallel conductors for the busbar system is of special interest as the electromagnetic force on them is usually high compared to transversal arrangements. The three-phase and line-to-line short-circuit without contact to ground normally generates the highest short-circuit current which causes maximum impact due to high electromagnetic force (Hairi, Zainuddin, Talib, Khamis, & Lichun, 2009; Schlabbach, 2005). Therefore, in this research work, it is essential to consider the three-phase short-circuit currents to produce the maximum electromagnetic force on a conductor busbar.

In this study, we investigate the relationship between short-circuit current and electromagnetic force that is concentrated on a three-phase rectangular copper

busbar. The bare conductor busbar is considerably exposed to stagnant air. The electromagnetic force produced between each conductor of busbar is calculated from the specific short-circuit current based on the IEC Standards. In addition, the studies on the relationship between transient short-circuit current and the electromagnetic force of copper busbar is carried out in a compact enclosure which involves flattened 3-phase 5-wire busbar placed in galvanized steel duct.

The magnetic flux distribution on the busbar system is simulated and the electromagnetic force produced is calculated. The estimated electromagnetic force is essential in predicting the performance of the busbar system under short-circuit currents. This finding is also useful to identify the appropriate dimension of busbar systems in order to guarantee the mechanical stability of the system due to short-circuit current (Kasikci, 2002).

1.2. Problem Statement

Like other electrical power system, busbar may face some problem due to electrical faultiness. Faults due to short-circuit in power system cannot be avoided despite good maintenance and thorough operation system. Therefore, short-circuit test is carried out to ensure the system design is able to carry its short-circuit current and withstand short-circuit electromagnetic force for a definite time. However, the facilities for short-circuit test in Malaysia are not available at the moment. The manufacturer is required to send their product to a country that provides such facilities in order to perform the short-circuit test. Furthermore, cost for performing the short-circuit test is very high and will continue to get higher if the tested product has failure. This is likely due to the manufacturers needs to repeat the test until the product has passed as well as reached the standard safety level. Therefore, in order to

overcome this problem, estimation of electromagnetic force on the busbar system under three-phase short-circuit current should be carried out before sending the system for testing. This helps the manufacturer to predict the performance of the busbar system against short-circuit current and also determine the appropriate design that able to withstand the effects of short-circuit currents. It is certainly better to spend extra attention in the design and the construction stages to provide maximum system performance under all conditions especially during short-circuit. Therefore, the probability of the system having failure under testing can be reduced. Some objectives are carried out in this research work to fulfill this purpose.

1.3. Objective

The objectives of this project are:

- i. To calculate the electromagnetic force of a bare conductor busbar under peak steady-state short-circuit current and compare with simulation results.
- ii. To estimate the electromagnetic force on a 3P5W busbar system under peak transient short-circuits current by finite element analysis.
- iii. To analyze the relationship between the configuration arrangement of a busbar system and the magnitude of an electromagnetic force.

1.4. Scope of Research

This project can be categorized into two major conditions of short-circuit current. For the first condition, determination of electromagnetic force is conducted towards the bare copper conductor busbar by applying steady-state three-phase symmetrical current. At this stage, the peak value of steady state AC current is assumed to be equal to the peak value of a short-circuit current. It involves the

calculation of a short-circuit current and an electromagnetic force. In this study we deal with a three-phase short-circuit current which had generated the highest short-circuit current thus giving the highest impact on the electromagnetic forces. The strength of a three-phase short-circuit current and their maximum electromagnetic force is calculated numerically based on IEC Standard 60909 and 60865, respectively.

The second condition involves simulation of a magnetic field distribution and the estimation of an electromagnetic force under a three-phase transient short-circuit current. Two-dimensional finite element is used in this simulation. The simulation is performed for different dimensions of a busbar system with different carrying currents in order to differentiate the relationship of busbar dimension to the electromagnetic force. The influence of the configuration of busbar system on the production of electromagnetic force against short-circuit current is also considered in this study. All analysis and simulation for these conditions are limited to a 3-phase 5-wire (3P5W) compact busbar system designed by Furutec Electrical Sdn. Bhd. Furthermore, a numerical calculation is performed to validate the simulation result.

1.5. Structure of Thesis

This thesis is organized into five main chapters.

Chapter 2 discusses in detail the past research trend related to the subject of this study. The literature reviews on this chapter are focused on a three-phase short-circuits current and an electromagnetic force on the conductor busbar. All the important equations and knowledge that were applied in the analysis are described in this chapter.

Chapter 3 describes in detail regarding the project flow of short-circuit electromagnetic force analysis. All relevant descriptions, theoretical and analytical techniques carried out throughout the research are shown in detail.

In Chapter 4, the calculation and simulation results of the short-circuit busbar system are presented. The result of electromagnetic force due to short-circuit current is divided into two majors conditions. Steady-state short-circuit current is applied for bare copper conductor busbar while transient short-circuit current is for 3P5W compact busbar system. Factors that influence the electromagnetic force is discussed in this chapter.

Lastly, Chapter 5 concludes the thesis content. The concluding remarks together with future works for this research are justified. Some recommendations for future research improvement are also stated at the end of this chapter.

1.6. Contribution

This research work is conducted to estimate the maximum electromagnetic force exerted on the conductor of the busbar system due to certain short-circuit current. By applying time stepping of finite-element method in transient analysis the instance when this maximum electromagnetic force occurs can be determined. This estimation of electromagnetic force also can be done at various type or design of busbar system. The factors that influence the electromagnetic force can be obtained at the end of this research. The estimation results of maximum electromagnetic force are very useful as fundamental knowledge for busbar system designers in order to predict the performance of the busbar against certain short-circuit current before sending for short-circuit testing.

CHAPTER 2

LITERATURE REVIEW

2.1. Introduction

This chapter provides the summaries of related research work and the interpretation of relevant background information required. The literature review is based on short-circuit electromagnetic force on busbar system including the factors that affects the electromagnetic force between the conductor busbar.

2.2. Research Trend on Electromagnetic Force due to Short-circuit Current

Busbar power distribution systems are rapidly gaining broader acceptance due to their flexibility, safety and ability to reduce overall design and integration costs. Originally the busbar system included bare copper or aluminum conductor supported on inorganic insulators, mounted within a grounded metal housing. In typical busbar systems the current-carrying conductors are usually placed parallel to each other. The electromagnetic force produced by parallel conductors is proportional to the products of their currents. Under normal operating conditions, the electromagnetic force is very small and does not give significant impact to its mechanical structure. However under short-circuit conditions, most busbar systems are subjected to permanent deformation or break of supporting structures if large electromagnetic force occurs due to carrying high short-circuit current. The estimations of maximum electromagnetic force on the three-phase busbar system is very important, especially to analyze its effect on the mechanical structure of busbar system.

The study of conductors to withstand short-circuit electromagnetic force is certainly not new as is shown by the number of publications which have raised this issue. Labridis and Dokopoulos (1996) have studied short-circuit electromagnetic force on three-phase rigid rectangular cross section busbar. The electromagnetic force was calculated at peak short-circuit current by assuming steady-state, balanced three-phase current with a peak value equal to the peak value of short-circuit current (Labridis & Dokopoulos, 1996). The electromagnetic force and current densities were calculated by solving the electromagnetic field diffusion equation numerically using finite elements. The result of computational short-circuits electromagnetic force were fully detailed with results calculated according to the IEC Standards 60865/86, as well as with the corresponding technical revision IEC 60865/93. Labridis et al, proved that the geometrical configuration and the profile of the conductors should not be neglected in order to take into account the force dependence. This is due to skin and proximity effects in low voltage system that cannot be neglected. It has evaluated the significance of suggesting the effective central distance a_m in IEC 60865/93, instead of directly using the centre-line distance a as in IEC 60865/86.

In the next few years, an extensive analysis had been done by Triantafyllidis, Dokopoulos, & Labridis (2003) onto the same design of conductor busbar as in Labridis and Dokopoulos (1996). Improvements have been made by solving the short-circuit computation using finite element method (FEM) covering a wide variety of cases in a large number of arrangements, as used in AC indoor installations of medium and low voltage (Triantafyllidis, Dokopoulos, & Labridis, 2003). Automatic mesh generation had been utilized by a let-it-grow artificial neural network (ANN). The forces calculated for all cases were in excellent agreement with the IEC Standard

60865/93. The new proposed technique made the convergence of the method faster and led to more accurate results than the meshes produced by the conventional meshing procedures for some cases.

Later, the concept of effective distance for the adjacent configuration introduced in the IEC Standard 60865/93 was fully detailed and a new concept had been developed regarding the nonadjacent conductors (Canova & Giaccone, 2009). Calculation of the electrodynamic effort in the system by an analytical method was a fast way but it has the limitation of assuming a constant current density in each massive conductor.

As reported from those researchers, short-circuit electromagnetic force of the conductor busbar was predicted from the peak short-circuit by assuming the peak of steady-state balanced AC current was equal to the peak of short-circuit current. However, short-circuit current characteristic can be made up of two components which are decaying DC transient and steady-state sinusoidal component where current remains after the decay of all transient phenomena. Transient electromagnetic force has been computed in several types of busbar. The peak value of short-circuit current should be known in order to estimate the maximum short-circuit electromagnetic forces of transient short-circuit current. This peak short-circuit current value depends on the time constant of the decaying DC transient component.

For the case of transient short-circuit current, Demoulias, Dokopoulos, & Tampakis (1985) have developed a three-phase transient current to analyze short-circuit current effect. A gas installed cable which consists of three phase conductors symmetrically arranged in a thin tubular shell for power transmission had been considered (Demoulias, Dokopoulos, & Tampakis, 1985). By considering to a three-

phase short-circuit far from generator, transient short-circuit current was imposed through phase conductors. Complex potential and space complex were applied to calculate the field and forces in the system. In order to signify the dependence of electromagnetic force, parameters like conductivity, cable dimensions and current asymmetry were varied.

In other research, analytical method had been developed for the field and force computation due to transient short-circuit force for three parallel and coplanar busbar (Dokopoulos & Tambakis, 1991). In this method, they used the complex potential and solved the Maxwell equations analytically. The thickness of enclosure was neglected and the conductor was assumed as current filaments. This method caused a significant reduction of computation accuracy. This analysis involves the technical arrangements of coplanar busbar with and without shell. It seems that the arrangement with shell reduced the force applied on the phase conductor by a factor of 20 or more compared with the arrangement without shell. The effects of conductor distance on the maximum forces considered in this work were analyzed. However, the analytical model used for the system is over-simplifications where the maximum force was developed had not been investigated. In fact, this instance was essential especially in determining the response time of protection system.

Thus, a major study done by Isfahani et al. found that the time-stepping FEM had been employed to overcome the problem associated with the approximated analytical models (Isfahani & Vaed-Zadeh, 2007; Isfahani & Vaez-Zadeh, 2008; Isfahani, Vaez-Zadeh, & Khodabakhsh, 2009). This FEM based program was developed which provides easy determination of maximum force on the system under the worst condition. The effects of different system specifications on the maximum value of force and the instance at which this force occurs were

investigated. The results showed that the instance of force occurs do not change in most cases; except the value of maximum force. Only the current phase angle and enclosure permeability affects the occurrence time of maximum force. The characteristic of force affected from the variable conductors distance and the type of enclosure materials implemented for the system were also considered. The overall results were useful for the design and protection of the buses system.

From the literature review, it is understood that the key parameter to predict the maximum short-circuits electromagnetic force is the magnitude of three-phase short-circuit current. This three-phase short-circuit current contributes to the highest effects of electromagnetic force on the conductor busbar as compared to other short-circuit current types such as line-to-line short-circuit current, line-to-earth short-circuit. Furthermore, to ensure the system design is safe and able to operate properly it must be capable to successfully operate under three-phase short-circuit current without causing any failure and damage to the structure. This fact is based on the short-circuit test report provided by the manufacturer. Therefore, for this research work it is essential to estimate the electromagnetic force under three-phase short-circuits current so that it will help to predict the performance of the system before sending for testing. In this research work, electromagnetic force on rigid bare conductor busbar is estimated under steady-state current where the peak current is equal to the peak three-phase short-circuits current. Then, it is followed by analysis 3P5W busbar system arranged in compact galvanized steel enclosure under transient short-circuits current. In addition, the effects of different specification of conductor busbar on the magnitude of electromagnetic force generated were investigated. Numerical calculation is presented in order to validate the estimation result of electromagnetic force from the simulation.

2.3. Related Theory of Short-circuit Current

A three-phase power system has to be distinguished between different types of short-circuits. This short-circuit can be classified to the following types (2001 Geneva: IEC, 2001; Sang, 2003):

- i. Three-phase short-circuit - short-circuit of all three-phases
- ii. Line-to-line short-circuit with earth connection - short-circuit between any two phases and earth
- iii. Line-to-line short-circuit - short-circuit between any two phases
- iv. Line-to-earth short-circuit - short-circuit between any phase and earth

Maximal short-circuit current is the main design criteria for the rating of equipment in order to withstand the effect of short-circuit current, i.e., thermal and electromagnetic effect (Schlabach, 2005). Three-phase short-circuit current must always be considered in this case study since this type of short-circuit current normally gives the highest impact of electromagnetic force on the electrical equipment.

2.3.1. Three-phase Short-circuit Current

The three-phase short-circuit is a symmetrical short-circuit which the magnitude is balanced equally within the three phases. This short-circuit type generally yields the maximum short-circuit current values. Figure 2.1 provides a graphical representation of three-phase short-circuit current for positive sequence network where I_{k3}'' is for initial symmetrical three-phase short-circuit current and Z_I , I_I and $cU_n/\sqrt{3}$ represented for current, impedance and equivalent voltage source introduced at short-circuit current location (Davis et al., 2006; Kasicki, 2002).

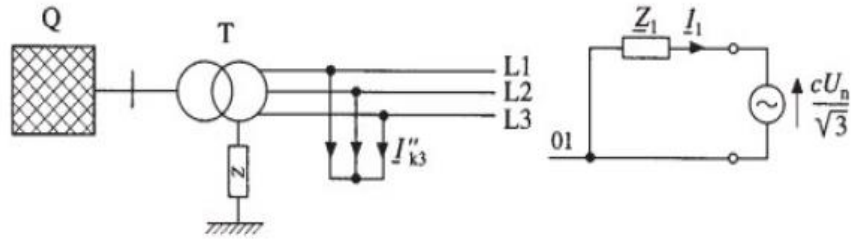


Figure 2.1: Equivalent circuit for a three-phase short-circuit (Kasikci, 2002)

2.3.2. Initial Symmetrical Short-circuit Current I_k''

The initial symmetrical short-circuit current is calculated for balance and unbalanced short-circuits based on the equivalent voltage source at the short-circuit location. The short-circuit impedance that was referred to the short-circuit location should be determined by a system of symmetrical components. For the three-phase short-circuit current the initial symmetrical short-circuit current shall be calculated by the following equation, (2001 Geneva: IEC, 2001; Kasikci, 2002; Schlabbach, 2005)

$$I''_{k3} = \frac{c \cdot U_N}{\sqrt{3} Z_T} \quad (2.1)$$

where:

c : voltage factor according to Table 2.1

U_N : nominal system voltage

Z_T : total impedance of the operational equipment

The voltage factor c of Equation (2.1) shall be calculated based on Table 2.1 by taking into account the differences between the voltage at the short-circuit location and the internal voltage system feeders due to voltage variation, etc. Assuming the voltage factor as per Table 2.1 will result to short-circuit currents on the safe side, that are higher than in the real power system (Schlabbach, 2005).

Table 2.1: Voltage factor c according to IEC 60909-0

Nominal system voltage, U_N	Voltage factor c for the calculation of maximal short-circuit current, c_{max}
LV: 100 V up to 1000 V (inclusive) (IEC 60038, Table 1)	
Voltage tolerance $\pm 6\%$	1.05
Voltage tolerance $\pm 10\%$	1.10

2.3.3. Peak short-circuit current i_p

Depending on the application of the results, it is of interest to know the root mean square (RMS) value of the symmetrical AC component and the peak value of short-circuit current following the occurrence of a short circuit. The peak short-circuit current i_p , is a maximal instantaneous value of short-circuit current which occurs approximately a quarter periods after the initiation of short-circuits. The current can be calculated for the different types of short-circuits based on the initial short-circuit current (RMS) value. For three-phase short-circuit current, the peak short-circuit current is illustrated by Equation (2.2) (2001 Geneva: IEC, 2001; Kasikci, 2002; Schlabbach, 2005)

$$i_p = k \cdot \sqrt{2} I''_{k3} \quad (2.2)$$

The initial short-circuit current I''_{k3} and the withstand ratio k determine the peak short-circuit current. The factor k depends on the ratio R/X of the short-circuit path. If the ratio of R/X is known, the factor k can be obtained from Figure 2.2 or calculated by the following equation (Kasikci, 2002; Schlabbach, 2005)

$$k = 1.02 + 0.98 \cdot e^{-3 \frac{R}{X}} \quad (2.3)$$

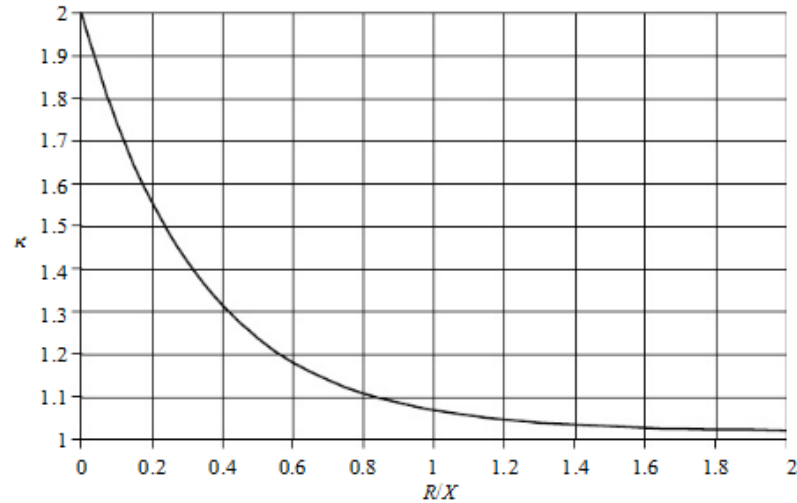


Figure 2.2: Factor k for the calculation of peak short-circuit currents (Schlabach, 2005)

In a short-circuit test, the value of a peak current can be obtained from the value of a RMS short-circuit current. The relationship between the peak and the RMS value of the prospective short-circuit current is defined by the coefficient of asymmetry n . These standards specify both the test conditions to be complied with and the standardized value of the coefficient connecting the peak value to the RMS value of the short-circuit current. In fact, this standardized value of the coefficient n is corresponding to coefficient $\sqrt{2}k$ as defined in Equation (2.2). The coefficient for factor n and the corresponding power factor are given in Table 2.2 (Killindjian, 1996).

Table 2.2: Standard values for the factor n

RMS value of short-circuit current (kA)	cos φ	n
$I \leq 5$	0.7	1.5
$5 < I \leq 10$	0.5	1.7
$10 < I \leq 20$	0.3	2.0
$20 < I \leq 50$	0.25	2.1
$50 < I$	0.2	2.2

A typical waveform which provides means of understanding the shape and the relation of short-circuit current term is shown in Figure 2.3. Following the decay of all transient phenomena, the steady state sets in. This short-circuit current characteristic can be measured at low-voltage installation in the vicinity of power stations (2001 Geneva: IEC, 2001; Kasikci, 2002; Metz-Noblat, Dumas, & Poulain, 2005; Sweeting, 2012)

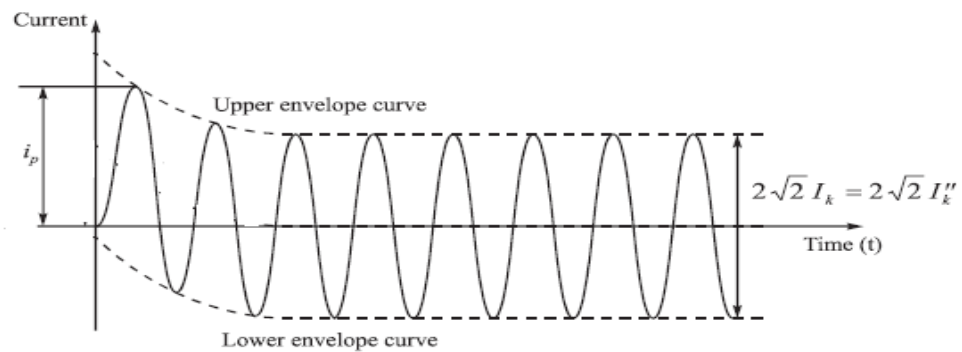


Figure 2.3: Time behavior of short-circuit current (Kasikci, 2002)

Where:

I_k'' : initial symmetrical short-circuit current

I_k : steady-state short-circuit current

i_p : peak short-circuit current

2.3.4. Development of Three-phase Short-circuit Current

A simplified network comprising of a constant AC power source, inductance L and resistance R is shown in Figure 2.4. When the switch is closed where no short-circuit is present, the design current I flows through the network. When short-circuit occurs between A and B, the negligible impedance between these points results in a very high short-circuit current that is limited only by R and L . The current develops under transient conditions depending on the reactance X and the resistance R (Metz-Noblat et al., 2005).

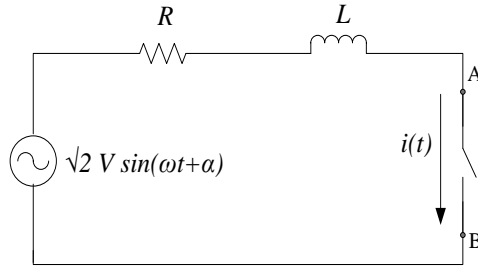


Figure 2.4: Equivalent single-phase diagram on three-phase short-circuit current

The following differential equation can be used to describe the short-circuit currents behavior as a function of time is involved (Davis et al., 2006; Kasikci, 2002; Killindjian, 1996; Metz-Noblat et al., 2005; Saadat, 2002):

$$Ri(t) + L \frac{di(t)}{dt} = \sqrt{2}V \sin(\omega t + \alpha) \quad (2.4)$$

where:

α : phase angle of the applied voltage at time of short-circuit (radians)

ω : $2\pi f$ where f is the system frequency (Hz)

If the current before short-circuit occurs is zero, the solution for Equation (2.4) is:

$$i(t) = \sqrt{2}I \left[\sin(\omega t + \alpha - \gamma) - e^{-t/\tau} \sin(\alpha - \gamma) \right] \quad (2.5)$$

where:

I : $\frac{V}{Z}$

Z : $\sqrt{R^2 + X^2}$

τ : $\frac{L}{R}$

γ : $\tan^{-1} \frac{\omega L}{R}$

All the factors representing the current variation as a function of time then grouped in the following equation (Killindjian, 1996; Metz-Noblat et al., 2005):

$$k = \left[\sin(\omega t + \alpha - \gamma) - e^{-t/\tau} \sin(\alpha - \gamma) \right] \quad (2.6)$$

The term k can also be calculated using the approximate formula defined by IEC 60909 as in Equation (2.3).

Figure 2.5 makes clear the importance and the range of applicability of short-circuit current calculations and additional calculations relating to other regulations. As electromagnetic force is proportional to the value of current, the peak short-circuits current should be known in order to calculate the maximum electromagnetic force affected on conductor busbar. For the case of short short-circuit duration, the short-circuit strength is well determined by the mechanical effects compared to the thermal effects of the short-circuit current (Kasicki, 2002; Ruger, 1989).

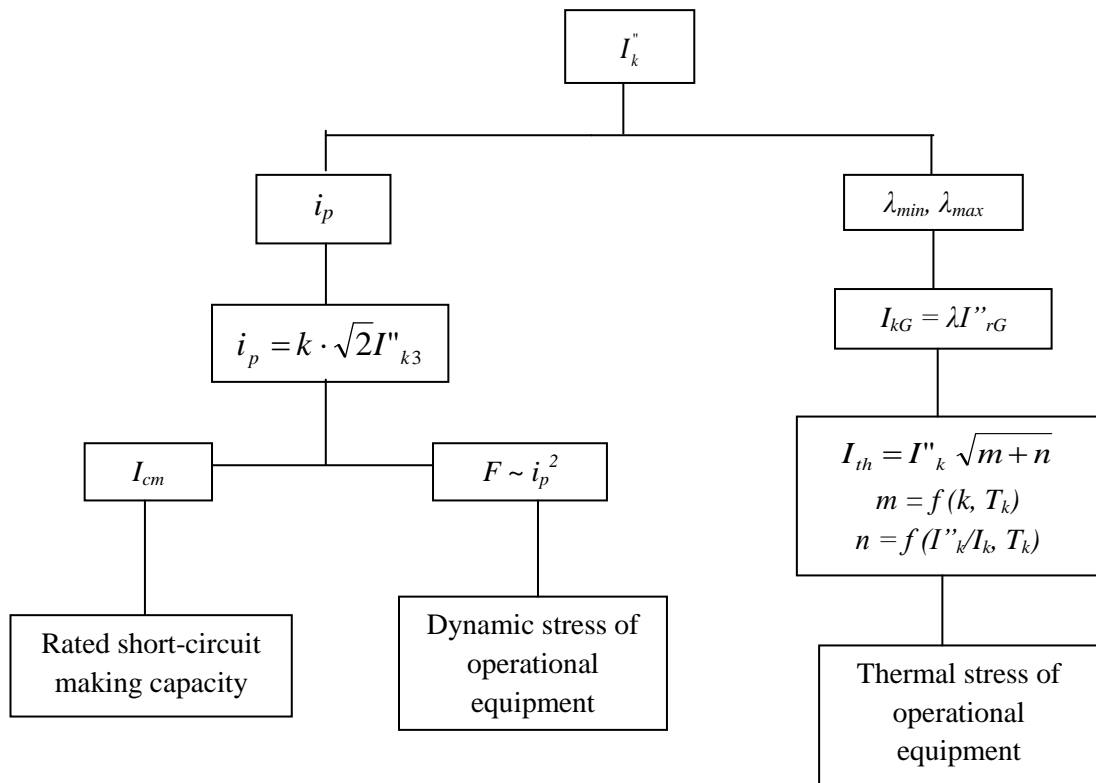


Figure 2.5: Range of applicability of short-circuit calculation (Kasicki, 2002)

2.4. Electromagnetic Force Affected by Short-circuit Current

The busbar system should be protected against short-circuit. The effect of electromagnetic forces acting on the conductor busbar with short-circuit current flowing is of great interest in this study. The arrangement of parallel conductor busbar gives a maximum electromagnetic force as compared to the transversal arrangement of the conductor busbar (Schlabach, 2005). Current flowing in conductors produce magnetic field and generate electromagnetic force.

2.4.1. Computational of Electromagnetic Force

Electromagnetic force acting on a current-carrying conductor depends on the magnetic flux density B , current intensity I and length l of the current-carrying conductors. The magnetic flux for a linear conductor can be calculated based on the Biot and Savart's Law as follows (Killindjian, 1996),

$$\vec{B} = \frac{\mu_0 I}{2\pi a} \quad (2.7)$$

When a current-carrying conductor of strength I in a magnetic flux B , the conductor is subjected to a Lorentz force. The electromagnetic force is calculated by applying the Laplace's law as follows (Killindjian, 1996; Lee, Ahn, & Kim, 2009). This electromagnetic force can be described mathematically by the vector cross product:

$$\vec{F} = i d\vec{l} \times \vec{B} \quad (2.8)$$

Considering two parallel conductors carrying currents I_1 and I_2 in the same direction, is separated by a distance a as shown in Figure 2.6. Denotes that B_1 is the magnetic flux due to current I_1 , defined at the location of conductor carrying the

current I_2 and B_2 is the flux due to I_2 at the location of conductor carrying current I_1 (Dawber, 2012). The magnetic flux B_1 and B_2 can be expressed as follows

$$\vec{B}_1 = \frac{\mu_0 I_1}{2\pi a} \quad (2.9a)$$

$$\vec{B}_2 = \frac{\mu_0 I_2}{2\pi a} \quad (2.9b)$$

The electromagnetic force exerted on each length of two parallel current carrying conductors is described as below

$$\vec{F}_1 = I_1 \times \vec{B}_2 \cdot l_1 = \frac{\mu_0 I_1 I_2}{2\pi a} l_1 \quad (2.10a)$$

$$\vec{F}_2 = I_2 \times \vec{B}_1 \cdot l_2 = \frac{\mu_0 I_1 I_2}{2\pi a} l_2 \quad (2.10b)$$

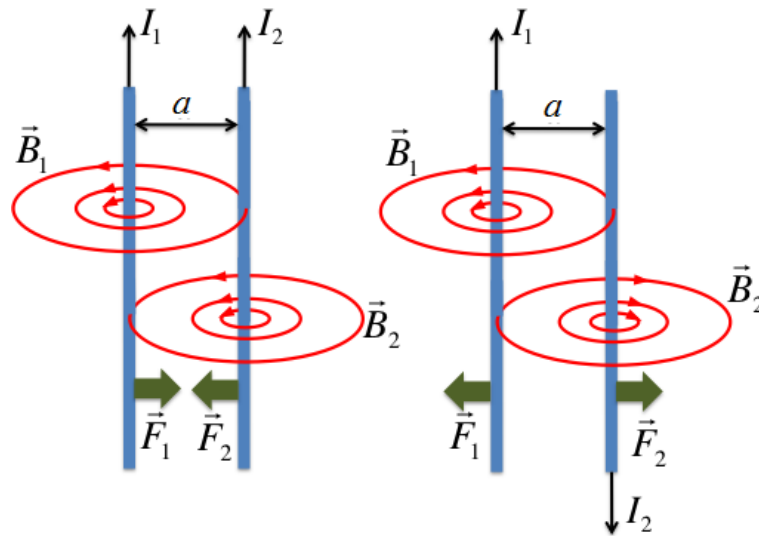


Figure 2.6: Effect of electromagnetic force acting on parallel current carrying conductor (Dawber, 2012)

The electromagnetic force exerted on both conductors is equal but react in opposite direction. If the current are in the same directions, the conductors will experience an attractive force with each other. Meanwhile, if both currents are flowing in opposite direction these two conductors will repel each other, whereby

these forces are distributed uniformly over the length of the conductors. The directions of force, conventional current and the magnetic flux are illustrated by Right Hand Grip Rule (Burley, Carrington, Kobes, & Kunstatter, 1996; Declercq, Adnani, & Lilien, 1996; Kasikci, 2002; Ulaby, 2005).

However electromagnetic force in Equation (2.10) only applies to current lines. In the case of solid conductor busbar, the influence of conductor shape may be determined by considering the cross section as a superimposition of interacting current lines. This approach was made by Dwight for a conductor with a rectangular cross-section (Killindjian, 1996; Metz, 1933). The resulting corrective factor conventionally denoted by k and can be determined in most cases on the S-shaped curves as in Figure 2.7.

The force per unit length exerted in air between the conductors is shown by assuming the current to be concentrated upon the centre lines. The equation then has the form:

$$\vec{F}_1/l = \frac{\mu_0 I_1 I_2}{2\pi} \left(\frac{k_{1s}}{a} \right) \quad (2.11)$$

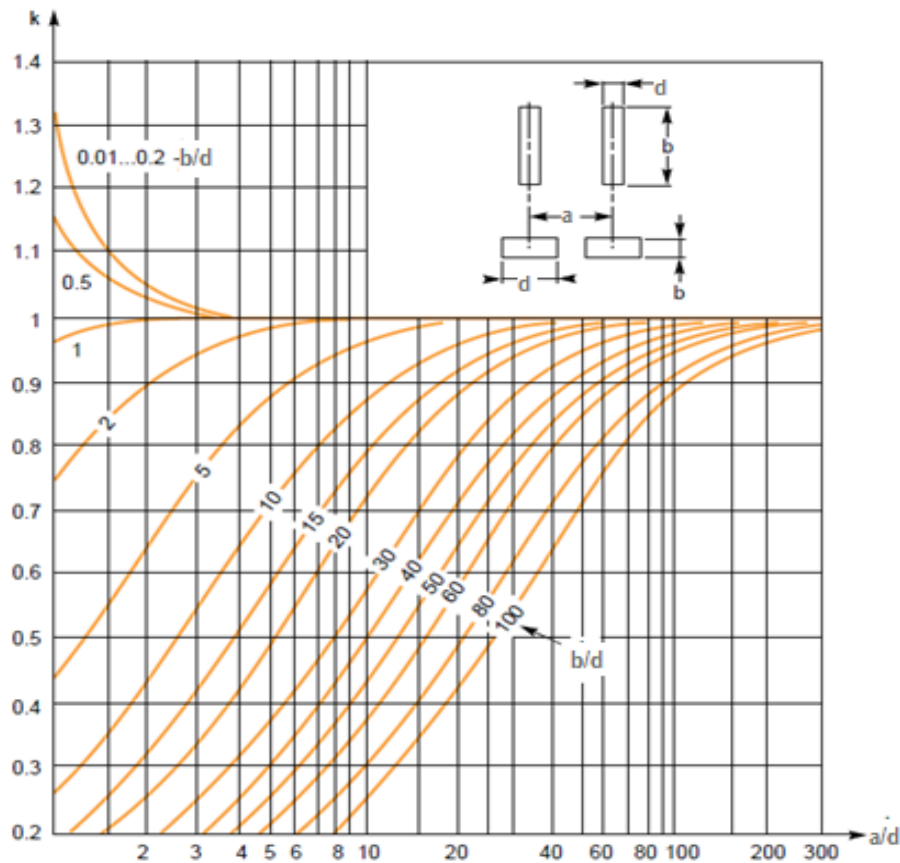


Figure 2.7: Variation of k_{1s} as a function of ratios a/d and b/d (Killindjian, 1996)

2.4.2. Calculation of Electromagnetic Force Based on IEC Standards 60865-1

Calculations method for the electromagnetic force caused by short-circuit current of three-phase AC systems is described exactly in IEC 60865-1 (1993 Geneva: IEC, 1993). Besides from the current strength and the configuration of conductors, the electromagnetic force between conductors also depend on the geometrical arrangement and the profile of the conductors (Shen, Zhang, & Zhou, 2009). This is due to the skin and proximity effect that cannot be neglected especially in low-voltage system. This fact has been proved by Labridis et al. in their research work (Labridis & Dokopoulos, 1996).

Instead of the central-line distance a , the effective distance a_m has been introduced in which the correction factor k_{1s} can be computed from Figure 2.7. This

factor is computed for a wide range of the geometrical parameters a , b and d (Declercq, Adnani, & Lilien, 1996; 1993 Geneva: IEC, 1993; Kasikci, 2002; Killindjian, 1996; Labridis & Dokopoulos, 1996; Triantafyllidis et al., 2003). The effective distance is expressed as follows

$$a_m = \frac{a}{k_{1s}} \quad (2.12)$$

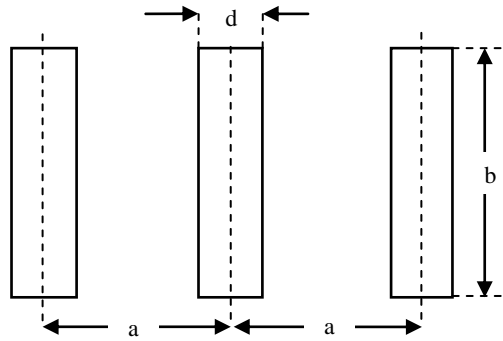


Figure 2.8: Cross-section of bare conductor busbar

Figure 2.8 shows the schematic diagram of a cross-sectional area of rigid bare conductor busbar. According to IEC Standards 60865/93, the maximum electromagnetic force per unit length acting on the central conductor is given by the following equation (1993 Geneva: IEC, 1993; Labridis & Dokopoulos, 1996)

$$F_{mb} = \frac{\mu_0}{2\pi a_m} \frac{\sqrt{3}}{2} i_p^2 \quad (2.13a)$$

While the maximum electromagnetic force for the outer conductor can be calculated as follow (1993 Geneva: IEC, 1993; Labridis & Dokopoulos, 1996)

$$F_{ma} = F_{mc} = \frac{\mu_0}{2\pi a_m} \frac{3+2\sqrt{3}}{8} i_p^2 \quad (2.13b)$$